Examination on safety factors in specifications

Coefficients de sécurité dans les spécifications

M. MATSUO, Professor of Geotechnical Engineering, Nagoya University, Nagoya, Japan
H. SUZUKI, Research Associate, Nagoya University, Nagoya, Japan

SYNOPSIS The specifications for design have been performing the important role in construction of the earth structures. The recent Japanese economic conditions in the low growth rate, however, require more severely the optimum decision of the safety factor in design. The safety factors to be applied to design of embankments and cut of slopes are investigated from the view point of reliability-based design. The results of analyses of some actual cases and many numerical examples for Japanese express highways suggest that the safety factors generally used in design of embankments on saturated clay layers lie in the reasonable level, while a little more delicate provisions might be required in design of embankments and cut of slopes at the mountainous districts.

INTRODUCTION

The present paper examines the safety factors in Japanese design specifications for the embankment and slope stability problems from the view point of reliability-based design. The safety factors for design should be said the fruit of the engineers' ample experience and they are expected to be in the reasonable level as a whole, but the theoretical demonstration has been strongly required by the final decision makers of the projects. In such a recent situation, it has become significant for engineering practice to newly evaluate the safety factors quantitatively by using the statistical decision theory with a loss function. In the present paper, the safety factors to be applied to design of embankments and cut of slopes are investigated by many numerical examples and the actual cases. As a result, it is shown that the decided optimum central safety factors of embankments on saturated clay layers are plotted closely by the level of the safety factors in the design specifications although the geometrical and mechanical conditions are different in each case, while a little more minute provisions for the safety factors might be required in design of embankments and cut of natural slopes for an express highway at a mountainous district.

OPTIMIZATION OF DESIGN

Stability Analysis

(a) Embankment on saturated clay layer: Failure of an embankment is caused by slide in a clay layer. The undrained strength $c_u(z)$ of a saturated clay layer is given by Eq. (1) as a random variable (Matsuo, 1976):

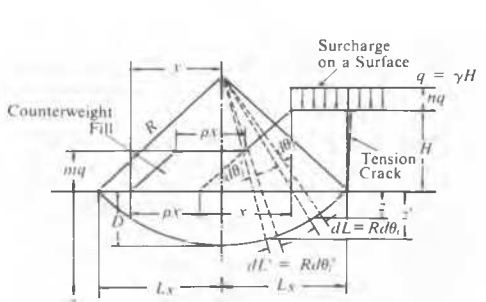

Fig. 1 Cross Section and Symbols of Embankment

$$c_u(z) = (\bar{c}_0 + kz) + (\sigma_0 + \kappa z)u(z) \tag{1}$$

in which z denotes the depth, $\bar{c}_0$ the undrained strength at $z = 0$, σ_0 the standard deviation at $z = 0$, $u(z)$ the standardized normal random variable at z and k and κ the increasing rates (constants) to z of the mean and the standard deviation, respectively. The stability analysis of an embankment with counterweight fill was already published (Matsuo and Suzuki, 1983-a) and only the final results are shown here. The central safety factor $\bar{G}$ which is the mean of the safety factor G as a random variable is expressed by using the symbols in Fig. 1:

$$\bar{G} = [2t^3/(c_1t^2 - c_2\rho^2 - c_3\rho - c_4)]\{(kx/\bar{c}_0) \times \{(\bar{c}_0/L_xk) - 1/\theta - \cot\theta\}(\theta/\sin^2\theta)(\bar{c}_0/q) \tag{2}$$

TABLE 1
Conditions for Calculations

$c_1 = (1 + n)/2 \qquad c_2 = m(1 + n - m)/[2(1 + n)]$

$c_3 = m(1 + 2n - m - mn)/[2(1 + n)] \qquad c_4 = (1 + 4n)/[24(1 + n)]$ (a)

$$t^2 = \frac{c_2\rho^2 + c_3\rho + c_4}{2c_1\left(\frac{1}{\theta} - \cot\theta\right)}\left|4\left(\frac{\bar{c}_0}{L_xk}\right) + 6\left(\frac{1}{\theta} - \cot\theta\right)\right| \tag{b}$$

$$\frac{\bar{c}_0}{L_xk} = \frac{3(\sin\theta - \theta\cos\theta) - \theta\sin\theta\tan\theta}{(\sin\theta + \theta\cos\theta)\tan\theta - 3\theta\sin\theta} \tag{c}$$

$$\left(\frac{x}{D}\right)^2 = \frac{c_1\sin\theta(2\theta\cos\theta - \sin\theta)}{(c_2\rho^2 + c_3\rho + c_4)(1 - \cos\theta)[2\theta\sin\theta - (1 - \cos\theta)]} \tag{d}$$

$$\beta > \alpha > \alpha_0 = \arctan|H_{max}\tan\beta_0/(H_{max} - B\tan\beta_0)| \tag{e}$$

$$\beta > \beta_0 \tag{f}$$

$$R \leqq |\tan\beta_1(B + R\sin\psi_3) - R\cos\psi_3 - H_S\tan\beta_1|/\sqrt{\tan^2\beta + 1} \tag{g}$$

$$f(\alpha,\theta|H_S, H, \beta_0, \beta) = \tan\beta_0[6(\sin\psi_{max} - \sin\psi_1) + 2(\sin3\psi_1 - \sin3\psi_{max})] + 3(\cos\psi_3 - \cos\psi_{max}) + \cos3\psi_3 - \cos3\psi_{max} + 3(\tan\beta_0\sin\psi_1 + \cos\psi_2)(\cos2\psi_{max} - \cos2\psi_1) + 3|2\sin\alpha\sin\theta - \tan\beta_0(\sin\psi_{max} - \sin\psi_1) + \cos\psi_2 - \tan\beta\sin\psi_3|(\cos2\psi_1 - \cos2\psi_3)$$ (h)

$$g(\alpha,\theta|H_S, H, \beta_0, \beta) = \tan\beta_0[4(\cos\psi_1 - \cos\psi_{max}) + \cos3\psi_1 - \cos3\psi_{max}] + 9(\sin\psi_{max} - \sin\psi_1) + \sin3\psi_{max} - \sin3\psi_1 + 9(\sin\psi_1 + \sin\psi_3) + 3(\tan\beta_0\sin\psi_1 + \cos\psi_2)(2\psi_1 - 2\psi_{max} + \sin2\psi_1 - \sin2\psi_{max}) + \sin3\psi_1 + \sin3\psi_3 + \tan\beta[3(\cos\psi_3 - \cos\psi_1) + \cos3\psi_3 - \cos3\psi_1] + 3|\tan\beta\sin\psi_3 - \cos\psi_2 - 2\sin\alpha\sin\theta + \tan\beta_0(\sin\psi_{max} - \sin\psi_1)|(2\psi_1 + 2\psi_3 + \sin2\psi_1 + \sin2\psi_3)$$ (i)

$$I_1 = \cos\psi - \cos\psi_2^* \qquad (\psi_1^* \leqq \psi \leqq \psi^*_{max})$$

$$I_2 = \cos\psi + \tan\beta\sin\psi + \tan\beta\sin\psi_1^* - \cos\psi_2^* - 2\sin\alpha^*\sin\theta^* + \tan\beta_0(\sin\psi_{max}^* - \sin\psi_1^*) \qquad (\psi_2^* \leqq \psi \leqq \psi_1^*)$$ (j)

$$K_1(\alpha^*,\theta^*) = \frac{24\sin\alpha^*\sin\theta^*}{f(\alpha^*, \theta^*)} \qquad K_2(\alpha^*,\theta^*) = \frac{12}{f(\alpha^*, \theta^*)}$$ (k)

The coefficients and the parameters in Eq. (2) are given by Eqs. (*a*), (*b*) and (*c*) in Table I. In an actual ground, a comparatively stiff layer often exists at a shallow depth under a soft clay and the slip circle of giving the minimum safety factor comes in touch with the stiff layer. In this case, Eq. (3) is applied instead of Eq. (2):

$$\overline{G} = 2\theta\bar{c}_0/[\{c_1 sin^2\theta - (x/D)^2(1-cos\theta)^2(c_2\rho^2 + c_3\rho + c_4)\}q] \quad (3)$$

in which $(x/D)^2$ is given by Eq. (*d*) in Table I. Since the autocorrelation coefficient of $c_u(z)$ can be written as $r_C(\Delta z) = \exp(-A_C|z-z'|)$ (Matsuo and Asaoka, 1977), the parameters δ, λ and $\sigma^2_{\bar{C}}$ which determine the characteristics of variation of the safety factor G become as follows:

$$\left.\begin{aligned} \delta &= 4\theta^2/\int_{-\theta}^{\theta}\int_{-\theta}^{\theta} exp(-A_C|z-z'|)d\theta d\theta' \\ \sigma^2_G &= (\overline{G})^2(V_C)^2/\delta \quad (V_C = \sigma_0/\bar{c}_0) \end{aligned}\right\} \quad (4)$$

$$\left.\begin{aligned} \lambda &= 4\{c_0\theta + k(Rsin\theta - \theta cos\theta)\}^2 \\ &\quad /\int_{-\theta}^{\theta}\int_{-\theta}^{\theta}(\sigma_0 + \kappa z)(\sigma_0 + \kappa z')exp(-A_C|z-z'|)d\theta d\theta' \\ \sigma^2_G &= (\overline{G})^2/\lambda \end{aligned}\right\} \quad (5)$$

In the case of a ground improved by the sand compaction piles, $\overline{G}$ is obtained by the regression analyses (Matsuo and Suzuki, 1983-b):

$$\overline{G} = \beta_0 + \beta_1\cdot(x/H) + \beta_2\cdot\bar{c}_0 + \beta_3\cdot k + \beta_4\cdot a_s + \beta_5\cdot D \quad (6)$$

in which a_s is called the sand replacement ratio and $\beta_5 = 0$ corresponds to the case without a stiff layer under a soft clay. The values of $(\beta_1 \sim \beta_5)$ used in the later numerical examples are given in Table II. The parameters δ, λ and $\sigma^2_{\bar{G}}$ are the same to those in Eqs. (4) and (5).

(b) Cut of unsaturated natural slope: The slip circle and the symbols of presenting the geometrical conditions used in the stability analysis at cutting a natural slope are shown in Fig. 2. H_{max} is the height that a slip circle does not get beyond because of rapid change of a slope gradient or existence of a fault, for instance. The tip of a circle is assumed to cross the toe of a slope. The strength parameters c and $tan\phi$ in Coulomb's equation can be regarded as the random variables:

$$\left.\begin{aligned} c &= \bar{c} + \sigma_c u(z) \\ tan\phi &= \overline{tan\phi} + \sigma_{tan\phi} u(z) \end{aligned}\right\} \quad (7)$$

in which $\bar{c}$ and $\overline{tan\phi}$ denote the means and σ the standard deviation. The overturning moment M_o and the resisting moment M_R can be written by using the symbols in Fig. 2 as follows:

TABLE II
The Values of $\beta_0 \sim \beta_5$

	H(m)	β_0	β_1	β_2	β_3	β_4	β_5
(A)	8.0	−0.122	0.274	0.040	0.176	1.408	−0.008
(B)	8.0	−0.096	0.218	0.037	0.208	1.296	—

(A): Existence of Stiff Layer
(B): Non-existence of Stiff Layer

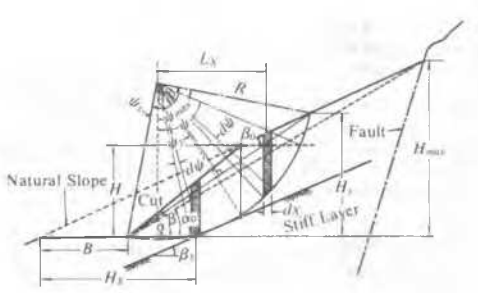

Fig. 2 Cross Section and Symbols of Cut

$$M_o = (\gamma R^3/12)f(\alpha,\theta|H_S,H,\beta_o,\beta) \quad (8)$$

$$M_R = cR^2(\psi_{max} + \psi_3) + (\gamma R^3 tan\phi/12)g(\alpha,\theta|H_S,H,\beta_o,\beta) \quad (9)$$

Eqs. (8) and (9) must satisfy three conditions (*e*), (*f*) and (*g*) in Table I and the contents of the functions $f(\cdot)$ and $g(\cdot)$ are given by Eqs. (*h*) and (*i*) in the same table. The geometrical condition (α^*, θ^*) minimizing $G(= M_R/M_o)$ can be determined by $(\partial G/\partial\alpha) = 0$ and $(\partial G/\partial\theta) = 0$. If H_S, H, β_0 and β in Eqs. (8) and (9) are given, the central safety factor can be calculated by the next equation:

$$\overline{G} = \{24\bar{c}(\psi_{max}^* + \psi_3^*)sin\alpha^* sin\theta^*\}/\{f(\alpha^*,\theta^*)\gamma H_r\} + g(\alpha^*,\theta^*)\overline{tan\phi}/f(\alpha^*,\theta^*) \quad (10)$$

Assuming that the autocorrelation function of $tan\phi$ is also written as $r_{tan\phi}(\Delta z) = \exp(-A_{tan\phi}|z-z'|)$, the parameters to characterize the variation of G become

$$\sigma^2_{\bar{G}C} = \sigma^2_{\bar{C}}\int_{\psi_3^*}^{\psi_{max}^*}\int_{\psi_3^*}^{\psi_{max}^*} exp(-A_C R^*|l_i - l_i'|)d\psi d\psi' \quad (i = 1,2) \quad (11)$$

$$\sigma^2_{\bar{G}tan\phi} = \sigma^2_{tan\phi}\int_{\psi_3^*}^{\psi_{max}^*}\int_{\psi_3^*}^{\psi_{max}^*} exp(-A_{tan\phi}R^*|l_i - l_i'|)l_i l_i' cos^2\psi cos^2\psi' d\psi d\psi' \quad (12)$$

and l_1 and l_2 are shown by Eq. (*j*) in Table I. Denoting the correlation coefficient by ρ, the covariance $\sigma^2_{\bar{G}}$ of the safety factor G is expressed by the following equation:

$$\sigma^2_G = \{K_1(\alpha^*,\theta^*)/\gamma H\}^2\sigma^2_{GC} + \{K_2(\alpha^*,\theta^*)\}^2\sigma^2_{Gtan\phi} + (2\rho/\gamma H)K_1(\alpha^*,\theta^*)K_2(\alpha^*,\theta^*)\sigma_{GC}\sigma_{Gtan\phi} \quad (13)$$

in which $K_{1,2}(\alpha^*, \theta^*)$ are given by Eq. (*k*) in Table I.

(c) Slide in embankment filled by unsaturated soils: By substituting $(\beta_0 = 0)$ and $(\psi_{max} = \psi_2)$ into Eqs. (*h*) and (*i*) in Tabel I,

$$\overline{G} = 48\bar{c}\theta^* sin\alpha^* sin\theta^*/\{f(\alpha^*,\theta^*)\gamma H\} + \{g(\alpha^*,\theta^*)/f(\alpha^*,\theta^*)\}\overline{tan\phi} \quad (14)$$

and other functions to be used are the same equations shown in the case of cut.

Calculation of Probability of Failure

The probability of failure P_F is given by the following equation (Matsuo and Asaoka, 1978):

$$P_F = P_{rob}[F = G + e \le 1] = \int_{-\theta_1}^{\theta_1}[1/\{(0.1) - (-0.1)\}]\int_{-\infty}^{1-\bar{G}-\epsilon}(1/\sqrt{2\pi}\sigma_G)exp(-G^2/2\sigma_G^2)dGde \quad (15)$$

in which e is the inevitable error of a design method itself and assumed as a random variable distributing uniformly in the range of $(-0.1 \sim 0.1)$ which is

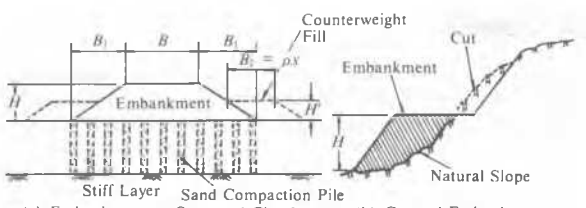

(a) Embankment on Saturated Clay Layer (b) Cut and Embankment (Unsaturated Slope)

Cost Functions

$$C_C = (B + 2B_1)c_a + H(B + B_1)c_b + 2B_2(c_a + c_bH') + C_{CP} \quad (i)$$

$$C_F = C'_C + C_R \quad C'_C = C_C \quad C_R = 500H\ (1000yen/m) \quad (ii)$$

$c_a = 6$ (1000yen/m^2) $c_b = 2.5$ (1000yen/m^3)
$C_{cp} = 3.45 \times$ (total length of constructed piles/m) (1000 yen/m)
c_a : Cost of Land to Purchase
c_b : Cost of Construction for a Unit Volume of an Embankment
C_{CP} : Cost of Construction of Sand Compaction Piles
C'_C : Reconstruction Cost of an Embankment
C_R : Incidental Cost Involving the Indemnity Cost

Fig. 3 Cross Sections and Cost Functions

based on the back analyses for the actual failure cases (Matsuo, 1976).

Evaluation of Design Alternatives

Denoting the set of parameters of distribution of the state of ground by $\theta = (\mu, \sigma^2)$, that of distribution of e by θ_e and the state of nature by $\underline{\theta} = (\theta, \theta_e)$, the loss function to evaluate the design alternatives can be written as follows (Matsuo and Asaoka, 1978):

$$L(\underline{\theta}, a^*) = \min_a [C_c(a)\{1 - P_F(\underline{\theta}, a)\} + C_F(a) P_F(\underline{\theta}, a)] \qquad (16)$$

in which $C_c(a)$ is the construction cost and $C_F(a)$ is the cost of failure. The optimum design a^* is obtained by minimizing the loss function (16).

DESIGN OF EMBANKMENT

Embankment on Saturated Clay Layer

The decided results of the optimum slope gradient of embankments, the optimum width of counterweight fills under the condition of $H' = 0.5H$ and the optimum sand replacement ratio (i.e. the diameter and the interval of sand compaction piles) of the improved soft ground are discussed. The illustration of a cross section is shown in Fig. 3(a) as well as the cost functions C_c and C_F. Each unit cost given in the figure is based on the recent actual embankments for express highways constructed in suburban areas in Japan. The results are plotted in Fig. 4 in which $\overline{G}^*$ is the optimum central safety factor. Fig. 4(a) is related to the optimum slope gradients of embankments without counterweight fills constructed on clay layers of various strength conditions of $k = \kappa = 0$ in Eq. (1). The improvement by sand piles are not carried out. The symbol s shows the equivalent shear stress on a slip circle. Fig. 4(b) corresponds to the cases of the couterweight fills and the improvement of soft grounds by sand piles. The former is based on the conditions that the embankment and the counterweight fill have the same given slope gradient and the soft grounds are not improved. In the latter, the embankments of the given slope gradient without counterweight fills are dealt with. The parameters k and κ are not zero in each case of Fig. 4(b). It is worthy of notice that the optimum central safety factors are almost plotted in the range of (1.2~1.35) which is the value used in the present general design in Japan, in spite of very different conditions of the ground strength and the construction methods of embankments. It is reasonable that $\overline{G}^*$ becomes large with the coefficient of variation of undrained strength V_C. Incidentally the probability of failure corresponding to $\overline{G}^*$ is about (1~3) percent.

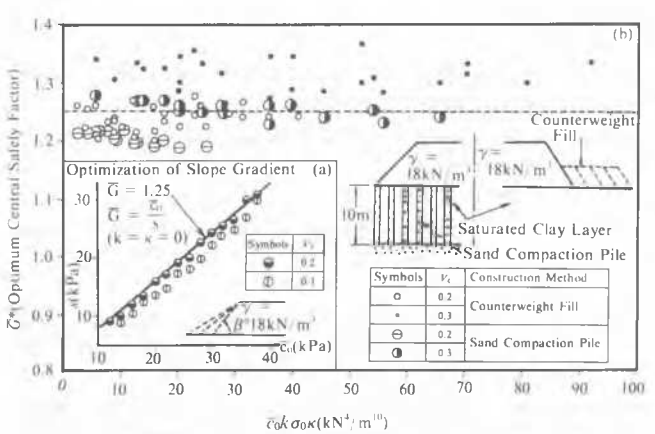

Fig. 4 Embankments on Saturated Clay Layers

Embankment for Express Highway of Mountainous District

The express highway in the moutainous region is often constructed by cutting the natural slopes and filling the cutted unsaturated soils (see Fig. 3(b)). In this case, there are three types of construction: (1) cut only, (2) cut at one side and embankment at the other side and (3) embankment only. The third type is investigated here and therefore Eqs. (i) and (ii) in Fig. 3 are applied to the loss function. The optimum solutions obtained by the reliability-based design are located in the shaded portion of Fig. 5. Since the coefficients A_C and $A_{\tan\phi}$ of the autocorretion functions are estimated to be (0~1.6) in the actual ground and embankment, both of the dotted lines can be said to show the extreme cases. The specifications of Japan Highway Public Corporation provide the slope gradient of embankment corresponding to its height under classification of soils and their strength. The specifications do not require the detailed stability analysis, but it is possible to calculate the safety factor for each case by applying the circular arc method. The result is shown by the solid line in Fig. 5. That is, this line can be regarded equivalent to the specifications. As can be seen from the figure, the present specifications give the close result to the optimum design. Although it is located in a little safe side compared with the optimum decision, this should be said reasonable under the very difficult circumstances of execution of the detailed soil investigations along a long line in the mountainous district. The safety factor in the specifications becomes very large in the small range of H. This is caused by the fact that the construction machines cannot make a slope too steep.

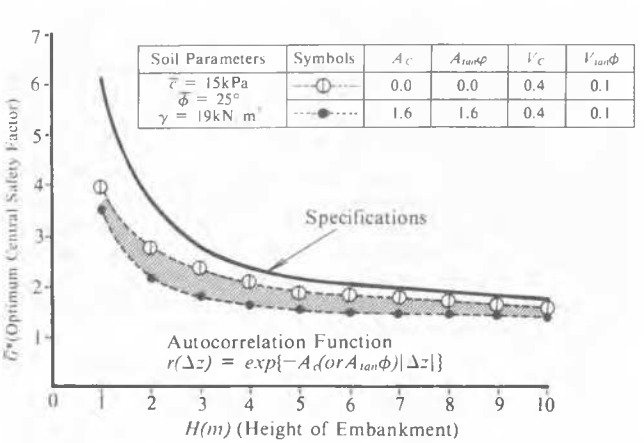

Fig. 5 Embankments by Unsaturated Soils

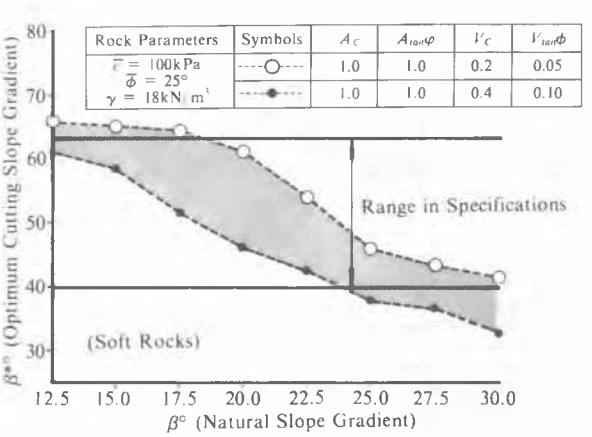

Fig. 6 Cut of Natural Slopes

CUT OF NATURAL SLOPE

Numerical Examples

The express highway at the mountainous region constructed by only cutting the natural slopes is investigated. This problem corresponds to the type (1) in the classification above stated. The specifications of Japan Highway Public Corporation are similar to the case of embankment. That is, the maximum slope gradient of cut is limitted to the cutting height for the kinds of soils and rocks of slopes. It does not control, however, the relation with the natural slope gradient β_0. The provided cutting slope gradient β is in the range of (40°~63°) in the case of the general soft rocks, for instance, which is given by two solid lines in Fig. 6. Two kinds of plotting marks in the figure show the optimum cutting slope β^* by the stability analysis. They have the extremely different variation of strength and therefore the optimum solutions concerning the general slopes are considered to lie in the shaded portion. The cost functions used in the reliability-based design are given by Eqs. (i) and (ii) in Fig. 7, but the cases without counterweight fill (i.e. $A_1c_1 = 0$) are calculated in Fig. 6. It can be seen from Fig. 6 that the results of the optimum decision are generally included in the range of the specifications.

Case Study

Fig. 8 shows the actual case. Four steps high cut was carried out in order to construct the express highway. Since the deformation of slope was observed right after cutting, the counterweight fill was constructed and the highway is used now. The first design of cutting slope followed the specifications and therefore it cannot be said unreasonable. The results of the reliability-based design applying the information from the soil investigations carried out at the design of counterweight fill are shown in Table III. The average gradient of the actual cutting slope was 41° as shown in Fig. 8. The optimum value β^* in Table III is about 39° and it is understood that the first design was located in a little unsafe side. The maximum width of the counterweight fill was limitted by 9.0 m in order to guarantee the effective width of the highway and the fill was carried out in 3.2 m height. As can be seen in Table III, the optimum height under the condition of the given width 9.0 m becomes (2.6~2.8) m. Since the counterweight fill was constructed after the sign of slide appeared, it is natural for the engineers to make the design a little safe.

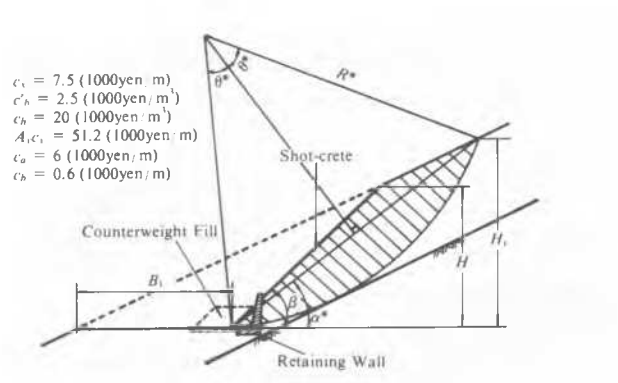

Cost Functions

$$C_C = (B_1 + H\tan\beta)c_a + 0.5B_1c_b + (H/\sin\beta)c_s \quad \text{(i)}$$

$$C_F = \{HR^*\sin\theta\sin(\beta - \alpha^*)/\sin\beta + (R^*)^2(\theta^* - \sin\theta^*\cos\theta^*)\}c'_b + A_hc_h + A_1c_1 + (H/\sin\beta)c_s \quad \text{(ii)}$$

c_s : Cost of Shot-crete of Slope
c'_b : Reconstruction Cost of Slope at Failure
A_hc_h: Cost of Retaining Wall
A_1c_1: Cost of Counterweight Fill

Fig. 7 Cross Section and Cost Functions

Actual Cutting Slope	Height Average Gradient	26m 41.1°
Counterweight Fill	Height Width	3.2m 9.0m

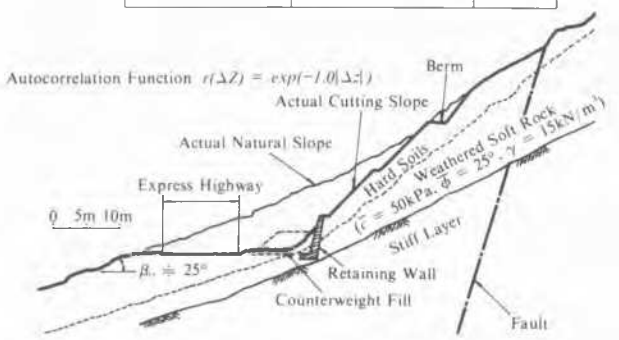

Fig. 8 Case Study of Cut of Natural Slope

TABLE III
Results of Optimization

Cutting Slope						Counterweight Fill				
V_C	$V_{tan\phi}$	$H^*_{(m)}$	$\beta^*_{(°)}$	$\bar{G}^*$	$P_F{}^*_{(\%)}$	V_C	$V_{tan\phi}$	$H'^*_{(m)}$	$\bar{G}^*$	$P_F{}^*_{(\%)}$
0.2	0.05	28.0	39.4	1.233	0.88	0.2	0.05	2.6	1.111	8.49
0.4	0.10	29.0	38.7	1.377	2.38	0.4	0.10	2.8	1.115	19.74

H^*, β^*: Optimum Height and Slope Gradient of Cut
H'^*: Optimum Height of Counterweight Fill

CONCLUDING REMARKS

The main remarks of the present paper are summarized as follows: (1) The optimum central safety factor decided by the reliability-based design of embankments on saturated clay layers becomes (1.2~1.35) which are the values used in the present general safety factor method. (2) The specifications for design of cut of natural slopes and embankments in the mountainous district give the fairly good results in comparison with the reliability-based design, but a little more delicate provisions might be required in future.

REFERENCES

Matsuo, M. (1976): Reliability in Embankment Design, MIT, Dept. of Civil Eng. Research Report, R76~33, pp.1~203.

Matsuo, M. and Asaoka, A. (1977): Probability Models of Undrained Strength of Marine Clay Layer, Soils and Foundations, Vol. 17, No. 3, pp.53~68.

Matsuo, M. and Asaoka, A. (1978): Dynamic Design Philosophy of Soils based on the Bayesian Reliability Prediction, Soils and Foundations, Vol. 18, No. 4, pp.1~17.

Matsuo, M. and Suzuki, H. (1983-a): Use of Charts for Reliability-based Design of Embankment on Saturated Clay Layer, Soils and Foundations, Vol. 23, No. 3, pp.13~26.

Matsuo, M. and Suzuki, H. (1983-b): Study on Reliability-based Design of Improvement of Clay Layer by Sand Compaction Piles, Vol. 23 No. 3, pp.112~122.